Response to anonymous referee #2:

Main Comments:

1.The identification of OA sources with PMF analysis could be improved. The authors could analyze how the factor mass spectra identified in the present study correlate with previous results. A library with existing profiles can be found here: https://cires1.colorado.edu/jimenez-group/HRAMSsd/.

In addition the mass spectra can be compared to unit mass resolution reference spectra from https://cires1.colorado.edu/jimenez-group/AMSsd/.

Reply: We thank reviewer to point this out. All resolved factors are now compared with literatures and the library reviewer suggested. Related discussions are now added.

"These POA had considerable fraction of hydrocarbon fragments (C_xH_y), indicating their less aged status. The HOA profile was characterized by higher contributions of aliphatic hydrocarbons and has dominated ion tracers such as *m/z* 41 ($C_3H_5^+$), 43 ($C_3H_7^+$), 55 ($C_4H_7^+$) and 57 ($C_4H_9^+$). The HOA concentration correlated with BC (r=0.62), which emits from traffic emissions. The diurnal variation exhibited strong morning and afternoon rush-hour peaks of mass concentration. This factor was consistent with the mass spectra of previously measured HOA from on-road vehicle emissions in urban cities (Zhang et al., 2005; Aiken et al., 2009; Sun et al., 2016; Hu et al., 2017), which has m/z peaks characteristic of hydrocarbon fragments in series of $C_nH_{2n+1}^+$ and $C_nH_{2n-1}^+$. The mass spectrum of HOA shows overall similarity to those of primary OA emitted from gasoline and diesel combustion sources (r=0.68) (Elser et al., 2016).

The OA from cooking sources (COA) is also characterized by prominent hydrocarbon ion series, however, with higher signal at $C_nH_{2n-1}^+$ than $C_nH_{2n+1}^+$. COA had apparent fragments of both $C_4H_9^+$ and $C_3H_3O^+$, and has a higher ratio of $C_3H_3O^+/C_3H_5O^+$ (3.1), $C_4H_7^+/ C_4H_9^+$ (2.2) than HOA (0.9–1.1), with cooking-related fragments of $C_5H_8O^+$ (m/z 84), $C_6H_{10}O^+$ (m/z 98) and $C_7H_{12}O^+$ (m/z 112) (Sun et al., 2011b; Mohr et al., 2012). The COA shows overall similar spectral pattern to the reference spectra of COA (r=0.92) (Elser et al., 2016). Its minor peak at noon and larger peak in the evening (Fig. 1l) also corresponded with the lunch and dinner time respectively."

"The BBOA factor was identified based on the prominent signals of *m/z* 60 ($C_2H_4O_2^+$) and 73($C_3H_5O_2^+$), which are known fragments of levoglucosan (Cubison et al., 2011). And BBOA also correlated with potassium (K^+, r = 0.80), which are indicator of biomass burning (Pachon et al., 2013; Brown et al., 2016). The *m/z* 60 and 73 together with a unique diurnal variation have been shown to be a robust marker for the presence of aerosols from biomass burning emissions in many urban locations (Sun et al., 2016). The BBOA shows very similar mass spectral patterns to previously reported reference spectra of biomass burning (r=0.94) (Elser et al., 2016). The BBOA factor that was identified in spring accounted for 12.8% of the total OA in Beijing, similar to previous reports (Hu et al., 2017). Biomass (Cheng et al., 2013) and solid fuel burning emissions (Sun et al., 2014) have been widely observed to importantly contribute to the primary OA in this region."

"Two types of oxygenated organic aerosols (OOA) were identified, in moderate (OOA2,

O/C=0.62) and high oxidation state (OOA1, O/C=0.95), respectively, which is very similar to the spectra of OOA factors resolved in other cities (Hayes et al., 2013; Ulbrich et al., 2009). The average mass spectrum of OOA2 in this study is characterized by *m/z* 29 (mainly CHO^+), 43 (mainly $C_2H_3O^+$) and *m/z* 44 (CO_2^+), similar to the semi-volatile OOA spectrum identified in other locations (Sun et al., 2011a; Zhou et al., 2016). On average, OOA2 accounts for 42% and 18% of $C_xH_yO^+$ and $C_xH_yO_2^+$ ions, respectively (Fig. 1b). These results clearly indicate that OOA2 was primarily composed of less oxygenated, possibly freshly oxidized organics. Notably, OOA2 had a substantially higher N/C than other factors (N/C=0.037), and had highest correlation with nitrate (r=0.77) and with $C_xH_yN_z$ and $C_xH_yN_zO_p$ fragments (r=0.83). This factor therefore tends to largely result from nitrogen-containing OA and its elevation at night may be also associated with dark oxidation by nitrate radical.

The mass spectrum of OOA1, which was characterized by a dominant peak at *m/z* 44 (mainly CO_2^+), a highest O/C (0.95). On average, OOA1 contributes 51% of the $C_xH_yO^+$ signal and 23% of the $C_xH_yO_2^+$ signal (Fig. 1a). OOA1 showed particularly high correlation with sulfate (r=0.40) because of their similar volatilities (Huffman et al., 2009; Jimenez et al., 2009)."

L166-168, L169-175, L176-178, L182-188, L195-199, L203-204

In addition, COA in previous works usually shows a peak at noon, while in this study the lunch peak is barely visible. The author should discuss this discrepancy.

Reply: The was only a minor peak at noon for COA, which may be due to the sub-urban nature of the site where the major aerosols from cooking sources may have been processed and lost the signature near source. Related discussions are now added:

"The was only a minor peak at noon for COA, which may be due to the sub-urban nature of the site where the major aerosols from cooking sources may have been processed and lost the signature near source. The feature of this factor was also observed in sub-urban environment (Huang et al., 2021)."

L179-181

Finally, the authors claim the use of external tracers to identify the PMF factors, but for COA an internal tracer was used instead, which makes the attribution risky, especially considering the correlation in time with HOA factors (based on the diurnal profile).

Reply: Previous literatures have widely used $C_6H_{10}O^+$ is considered a signature fragment mainly from cooking emission rather than from traffic (Sun et al., 2011b), but an unambiguous external tracer for cooking source is difficult to find. We have tested $C_6H_{10}O^+$ had a much weaker correlation with HOA (r = 0.48) than COA (r = 0.80), thus this factor is likely COA rather than HOA. In addition, the correlation between HOA and COA is 0.31 for time series, and 0.42 for mass spectra, therefore these factors can be discriminated.

2.This study identifies organic nitrate using ATR-FT-IR, integrating the spectra area around the characteristic absorption peaks at 860 cm^{-1} and 1640 cm^{-1}, in agreement with Liu et al. (2012). Nevertheless previous studies showed that the region between 1600 and 1700 cm^{-1}

shows typically a strong absorption signal due to the carbonyl group of ketones and carboxylic acid (Maria et al., 2002; Russell et al., 2009), which would lead to an overestimation of the NO_2 absorption at 1640 cm^{-1}.

Reply: We thank reviewer to point this out. Although the carbonyl group has absorption at 1640 cm^{-1}- 1850 cm^{-1} (Russell et al., 2009), and Maria et al. (2003) pointed out the absorption peak of carbonyl group was around 1720 cm^{-1}. However there was no discernable peak of carbonyl group for our infrared spectrum, and the peak of OH at 2500 cm^{-1} - 3400 cm^{-1} for the carboxylic acid is not discernable neither, thus the influence of ketone and carboxylic acid may be of less importance for our dataset. The related discussions are added.

"There was no discernable peak of carbonyl group for our infrared spectrum, and the peak of OH at 2500 cm^{-1} - 3400 cm^{-1} for the carboxylic acid is not discernable neither, thus the influence of ketone and carboxylic acid may be of less importance for our dataset."

L153-155

3.The discussion about the bleaching and darkening of BrC is based on the analysis of

diurnal profiles of primary and secondary BrC , both absolute absorption coefficient and fractional contribution in figure 4. The text reports: "Fig. 4b showed the decrease of primary BrC absorption tended to be more rapid than the HOA and BBOA mass (even a slight increase for HOA), which indicated the likely photobleaching process", but this decrease is difficult to discern in the figure.

Reply: A new plot about absorbing efficiency (absorption coefficient divided by mass) is now added in Fig. 4b to aid this conclusion. The related discussions are revised.

"Fig. 4b showed the decrease of primary BrC absorption tended to be more rapid than the HOA and BBOA mass (even a slight increase for HOA, Fig. 1m and Fig. 1o), leading to decreased absorption coefficient per unit mass of primary BrC (the shade in Fig. 4b), which indicates the photobleaching process."

L277-278

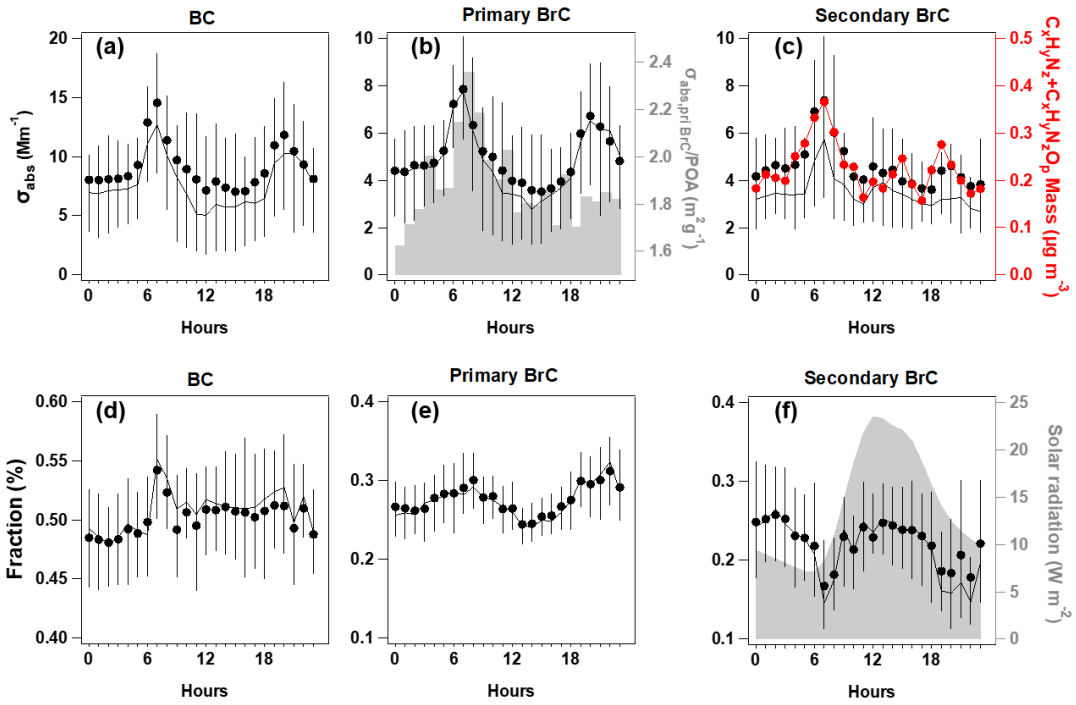

Figure 4. Diurnal variations of absorption coefficient at λ=375nm ($\sigma_{abs,375}$) for BC (a), primary BrC and the absorption efficiency of primary BrC ($\sigma_{abs,priBrC}$)/POA is shown in shade (b), and secondary BrC, along with the $C_xH_yN_z$ and $C_xH_yN_zO_p$ fragments (c); the respective fraction in total for the segregated $\sigma_{abs,375}$ (d-f), with direct radiation shown in shade. In each plot, the lines, dots and whiskers denote the median, mean and the 25th/75th percentiles at each hour respectively.

In addition, the attribution of secondary BrC to local photochemical production is based on the comparison between the fraction of secondary BrC diurnal profile and solar radiation, but if local photochemistry triggered secondary BrC formation I would expect to see a correlation between secondary BrC absorption (reported in fig.4 c) and solar radiation. On the contrary, secondary BrC absorption shows a peak in the morning, when photochemistry is expected to be lower.

Reply: We have carefully considered the comments from reviewer. The morning peak coinciding with the primary BrC can be explained as the rapid formation of BrC from sources when emitted gases rapidly condensed and formed aerosols. These may lead to high cooccurrence between primary and secondary BrC. Previous studies in urban environment also observed concurrent peaks of primary and secondary BrC, which usually occurred at morning rush hour (Zhang et al., 2020). In addition to the morning rush-hour peak, a peak after midday also observed for secondary BrC, and this small peak at noon was consistent with the peak of solar radiation, confirming that local photochemistry triggered the formation of secondary brown carbon. Related discussions are revised.

"The morning peak coinciding with the primary BrC may result from the rapid formation of BrC from sources when emitted gases condensed and formed aerosols. These may lead to high cooccurrence between primary and secondary BrC. Previous studies in urban environment also

observed concurrent peaks of primary and secondary BrC, which usually occurred at morning rush hour (Zhang et al., 2020).”

L271-274

Minor Comments:

1.Line 34-36. Please revise this sentence. Saleh et al. 2014 reported that the OA to BC ratio is higher during the smoldering phase, but do not compare the absorption efficiency of BrC produced during smoldering and flaming. Similarly, Chakrabarty et al. observed an increase in the absorption angstrom exponent of aerosol particles during smoldering, due to the larger OA contribution, but did not report differences in the imaginary part of the BrC refractive index during smoldering and flaming.

Reply: We have revised this sentence according to reviewer’s suggestion:

“These primary BrC had a range of absorptivity, which was found to be controlled by burning phases, with OA co-emitting with BC (the flaming phase) exhibiting a higher absorptivity than OA-dominated smoldering phase (Liu et al., 2021).”

L34-36

2.The authors classify the sampling period based on the analysis of back-trajectories (see figure S1). The sampling site is located in a suburban area of Beijing where local and nearby pollution sources are likely affecting the observed PM trend, rather than synoptic scale circulation. If the author wants to discriminate the sampling period into cluster, I would suggest to use local meteorology, including temperature, relative humidity, and wind speed/direction. For example, figure S1 shows an increase in the concentration and relative contribution of nitrate when relative humidity is higher, suggesting the relevance of local processes. Furthermore, wind speed and direction might help to spot the time when the impact of the urban Beijing area is higher.

Reply:

We thank reviewer to point this out. Local meteorology including wind and RH is also examined, which was found not to be the main driving factor to determine the pollution level, but the synoptic circulation of air mass is the major factor. This is because Beijing city acts strict environmental regulations but the air pollutants were synoptically transported from the polluted southern regions to the Beijing City, while the rapidly transported cleaner air from the north usually diluted the pollutants. The results here are consistent with a wide range of previous studies about the pollution conditions associated with synoptic patterns in Beijing region (Wu et al., 2022; Liu et al., 2019; Hu et al., 2020).

We have also included the local wind information in the revised figure S1.

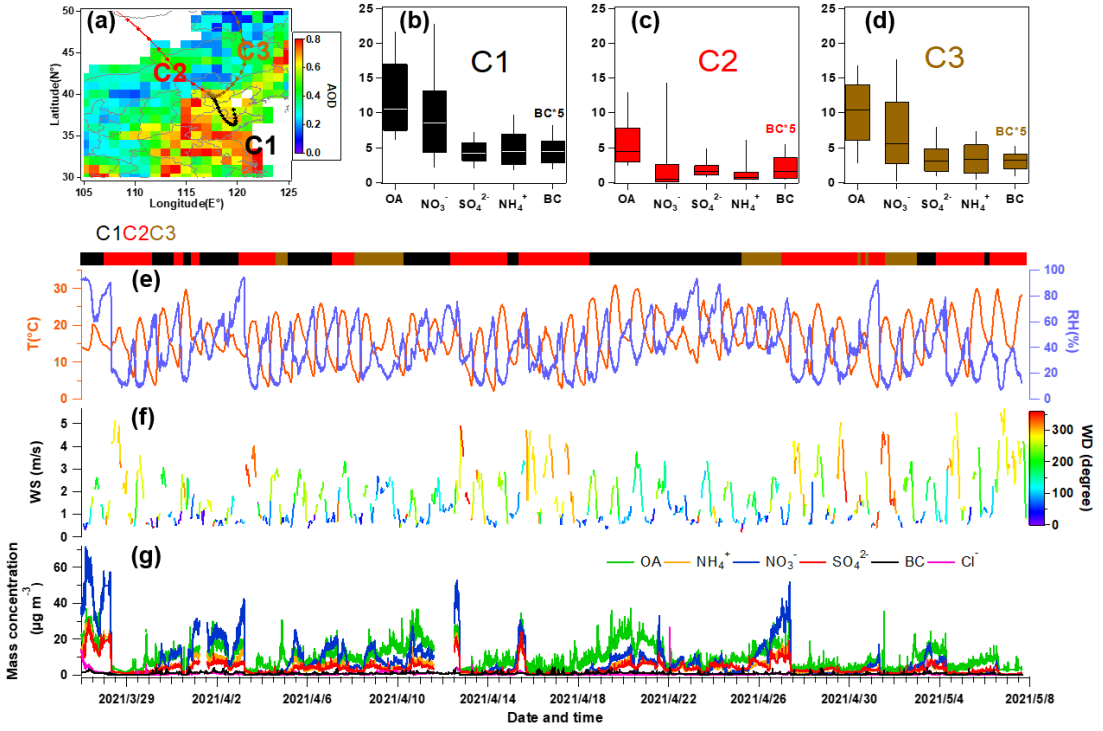

Figure S1. (a) Clustered back-trajectories for the past 72 hours during the experiment with markers denoting 12h intervals. (b-d) Statistics for the concentrations of key aerosol compositions from each cluster. The whiskers, box boundaries and lines in box denote the 10th/90th percentiles, 25th/75th percentiles and the median, respectively. (e) Time series of RH and T, (f) wind speed colored by wind direction, (g) mass concentrations of key aerosol compositions.

3.Line 77: the authors derived BC MAC based on the Mie theory. Liu et al 2018 showed that the Mie theory holds for spherical particles, but fails in reproducing the absorption of fractal particles. The author should discuss the uncertainty derived from it.

Reply: The coatings obtained by the SP2 measurement at λ=1064nm can be relatively independent of particle shape owing to the longer measurement wavelength, as discussed in previous studies (Liu et al., 2014; Hu et al., 2021). Related discussions are added.

"The SP2 measurement at λ=1064nm longer than mostly populated BC size means the derived coatings and subsequent calculation of MAC is relatively independent of particle shape within uncertainty of 21% (Liu et al., 2014; Hu et al., 2021)."

L83-85

4.Line 105: How do the primary absorption to rBC concentration ratios compared with previous studies?

Reply:

"The $\left(\frac{\sigma_{abs,total}}{[rBC]}\right)_{pri}$ ratio at λ=375 nm, 470 nm, 528 nm, 635 nm and 880 nm is calculated to

be 20.7, 17.0, 14.4, 11.7 and 5, respectively (Fig. S2), which falls within the reported values from previous studies 11-50 (Wang et al., 2019; Zhang et al., 2020)."

L117-118

5.Line 141-142: Inorganic nitrate usually dominates nitrate signal in the AMS measurements (Farmer et al., 2010). Please, revise this sentence or estimate organic nitrate from AMS signal and compare it with inorganic nitrate.

Reply: This sentence has been removed.

Technical comments:

Line 83: corrected instead of excluded

Line 181: constant instead of consistent

Line 226: accounted for instead of occupied

Reply: These are now corrected.

Figure1: the author might want to change the order of factors in the figure and report

OOA1 before OOA2.

Reply: This is revised.

Figure 3: If possible, the author might want to use horizontal lines instead of circles as markers in fig 3e to clarify that the FTIR data correspond to a time range of 24 hours. The horizontal lines should start and end at the beginning and end of the corresponding sampling period.

Figure 3: panel b shows a day dominated by secondary BrC at the end of the field experiment (likely May 7), while in fig 3c the secondary BrC absorption during the same day is not reported.

Reply: We thank reviewer to point this out. In Fig. 3, the missing data is now corrected and markers are revised according to reviewer's suggestion.

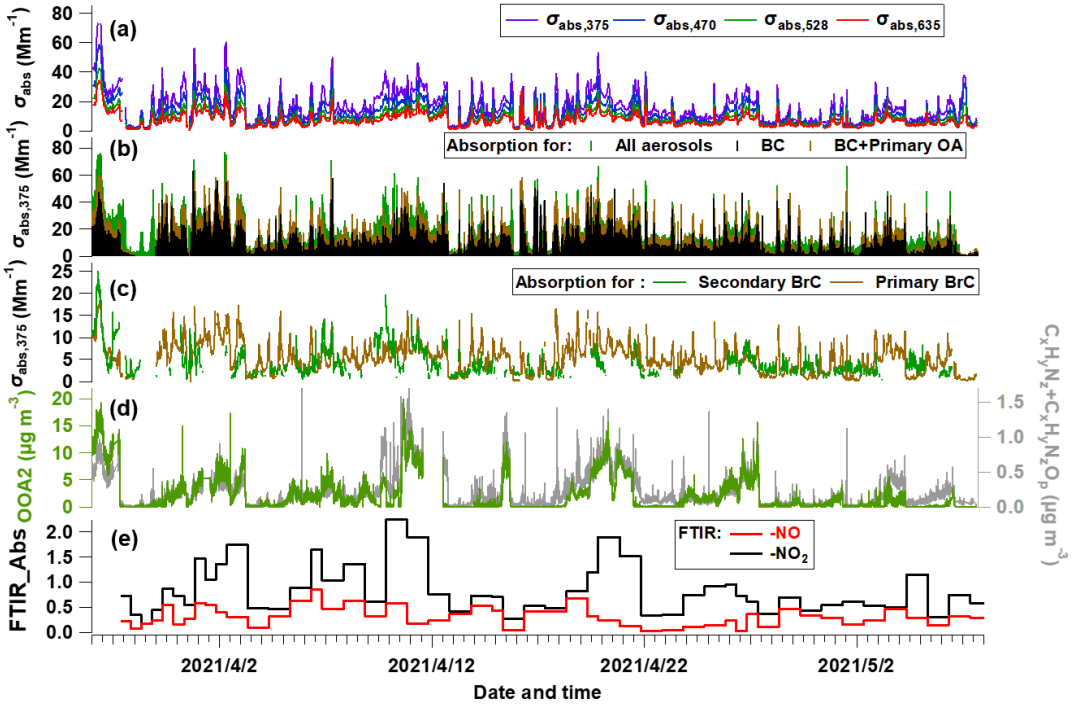

Figure 3. Temporal evolution of segregated absorbing properties. (a) Absorbing coefficients (σ_{abs}) at multiple wavelengths measured by the aethalometer, (b) σ_{abs} at λ=375nm ($\sigma_{abs,375}$) for all aerosols, primary OA and BC, (c) $\sigma_{abs,375}$ for primary BrC and secondary BrC. (d) mass concentration of OOA2 and the $C_xH_yN_z$ and $C_xH_yN_zO_p$ fragments measured by the AMS. (e) FTIR-measured absorption of -NO and -NO$_2$ bonds.

References

Hu, K., Zhao, D., Liu, D., Ding, S., Tian, P., Yu, C., Zhou, W., Huang, M., and Ding, D.: Estimating radiative impacts of black carbon associated with mixing state in the lower atmosphere over the northern North China Plain, Chemosphere, 252, 10.1016/j.chemosphere.2020.126455, 2020.

Hu, K., Liu, D., Tian, P., Wu, Y., Deng, Z., Wu, Y., Zhao, D., Li, R., Sheng, J., Huang, M., Ding, D., Li, W., Wang, Y., and Wu, Y.: Measurements of the Diversity of Shape and Mixing State for Ambient Black Carbon Particles, Geophysical Research Letters, 48, 10.1029/2021gl094522, 2021.

Liu, D., Allan, J. D., Young, D. E., Coe, H., Beddows, D., Fleming, Z. L., Flynn, M. J., Gallagher, M. W., Harrison, R. M., Lee, J., Prevot, A. S. H., Taylor, J. W., Yin, J., Williams, P. I., and Zotter, P.: Size distribution, mixing state and source apportionment of black carbon aerosol in London during wintertime, Atmos Chem Phys, 14, 10061-10084, 10.5194/acp-14-10061-2014, 2014.

Liu, D., Joshi, R., Wang, J., Yu, C., Allan, J. D., Coe, H., Flynn, M. J., Xie, C., Lee, J., Squires, F., Kotthaus, S., Grimmond, S., Ge, X., Sun, Y., and Fu, P.: Contrasting physical properties of black carbon in urban Beijing between winter and summer, Atmos Chem Phys, 19, 6749-6769, 10.5194/acp-19-6749-2019, 2019.

Maria, S. F., Russell, L. M., Turpin, B. J., Porcja, R. J., Campos, T. L., Weber, R. J., and Huebert, B. J.: Source signatures of carbon monoxide and organic functional groups in Asian Pacific Regional Aerosol Characterization Experiment (ACE-Asia) submicron aerosol types, Journal of Geophysical Research-Atmospheres, 108, 10.1029/2003jd003703, 2003.

Russell, L. M., Takahama, S., Liu, S., Hawkins, L. N., Covert, D. S., Quinn, P. K., and Bates, T. S.: Oxygenated fraction and mass of organic aerosol from direct emission and atmospheric processing measured on the R/V Ronald Brown during TEXAQS/GoMACCS 2006, Journal of Geophysical Research-Atmospheres, 114, 10.1029/2008jd011275, 2009.

Sun, Y. L., Zhang, Q., Schwab, J. J., Demerjian, K. L., Chen, W. N., Bae, M. S., Hung, H. M., Hogrefe, O., Frank, B., Rattigan, O. V., and Lin, Y. C.: Characterization of the sources and processes of organic and inorganic aerosols in New York city with a high-resolution time-of-flight aerosol mass apectrometer, Atmospheric Chemistry and Physics, 11, 1581-1602, doi:10.5194/acp-11-1581-2011, 2011b.

Wu, Y., Liu, D., Tian, P., Sheng, J., Liu, Q., Li, R., Hu, K., Jiang, X., Li, S., Bi, K., Zhao, D., Huang, M., Ding, D., and Wang, J.: Tracing the Formation of Secondary Aerosols Influenced by Solar Radiation and Relative Humidity in Suburban Environment, Journal of Geophysical Research-Atmospheres, 127, 10.1029/2022jd036913, 2022.

Zhang, Q., Shen, Z., Zhang, L., Zeng, Y., Ning, Z., Zhang, T., Lei, Y., Wang, Q., Li, G., Sun, J., Westerdahl, D., Xu, H., and Cao, J.: Investigation of Primary and Secondary Particulate Brown Carbon in Two Chinese Cities of Xi'an and Hong Kong in Wintertime, Environmental Science & Technology, 54, 3803-3813, 10.1021/acs.est.9b05332, 2020.